SRNL-STI-2025-00041

Proceedings of the ASME 2025
Pressure Vessels & Piping Conference
PVP2025
July 20-25, 2025, Montreal, Quebec, Canada

PVP2025-154678

Recent Advances in Pipeline Integrity for Transporting Blended Hydrogen-Natural Gas

Joshua Herrington, Xian-Kui Zhu, Bruce Wiersma
Materials Technology and Energy Science
Savannah River National Laboratory
Aiken, SC 29808, USA

ABSTRACT

To achieve US decarbonization goals, hydrogen is being considered as an alternative energy source to reduce carbon emissions. Blending hydrogen into existing natural gas pipelines is an intuitive first step to enable near term emission reductions. However, there are numerous challenges and uncertainties that complicate the transition to transporting hydrogen long-distance through existing natural gas pipelines. The main challenge is hydrogen embrittlement (HE), which reduces the ductility, fracture toughness and fatigue resistance of pipeline steels. This work delivers a technical review on HE effects on the material properties of pipeline carbon steels, such as Grade B, X52, X65, X70, X80, and X100. An important aspect of laboratory tests to capture the HE effect is the hydrogen test environment. This includes hydrogen pre-charged specimens tested in air and specimens tested in a hydrogen gas environment. A review of the mechanical properties of pipeline steel in different hydrogen environments determined through tensile testing is given first, which includes HE effects on yield strength, ultimate tensile strength, and ductility for blended hydrogen-natural gas pipelines. Then, the HE effects on fracture toughness and fatigue crack growth resistance are discussed. Last, impacts of HE to pipeline integrity and major technical challenges are discussed.

KEYWORDS: Hydrogen Embrittlement, Pipeline Steels, Tensile strength, Fracture toughness, Fatigue crack growth resistance

NOMENCLATURE

ΔK	Stress Intensity Factor Range
b	Finite Volume of Gas Molecules Constant
C_{OR}	Sub-surface Hydrogen Concentration
CT	Compact Tension
CTOD	Crack Tip Opening Displacement
DC	Direct Current
DSCT	Disk-shaped Compact Tension
FCGR	Fatigue Crack Growth Rate
f_{H_2}	Hydrogen Fugacity
HAZ	Heat Affected Zone
HE	Hydrogen Embrittlement
HEDE	Hydrogen Enhanced Decohesion
HELP	Hydrogen Enhanced Localized Plasticity
J_{IC}	J-integral based Elastic-Plastic Fracture Toughness
J_{IH}	J-integral based Elastic-Plastic Fracture Toughness measured in Hydrogen
J_Q	Apparent Initial Fracture Toughness
J-R	J-integral based Crack Growth Resistance Curve
K_{IC}	Plane Strain Fracture Toughness
K_{JH}	Plane Strain Fracture Toughness in Hydrogen converted from J-integral
K_{JIC}	Elastic-Plastic Fracture Toughness from J-integral
n	Strain Hardening Exponent
p_H	Partial Pressure of Hydrogen
p_T	Total Pressure
R	Universal Gas Constant
RT	Room Temperature
S	Sieverts Proportional Constant
SENB	Single-edge Notched Bend
SENT	Single Edge Notch Tension
T	Absolute Temperature
UTS	Ultimate Tensile Strength
YS	Yield Strength

1. INTRODUCTION

The United States (US) has set goals to create a carbon-free power sector by 2035 and then obtain net-zero carbon emissions no later than 2050 [1]. To accomplish these goals, there is a strong push to transition to using clean, carbon-free hydrogen as a replacement of fossil fuels in the high impact industrial, transportation and power sector applications. One limiting factor is the transportation of hydrogen gas at an affordable rate from where it is produced to the end users. The most cost-effective way to transport hydrogen gas is through steel pipelines. However, there is only approximately 1600 miles of hydrogen pipelines in operation in the US, which would not provide adequate distribution [2]. One alternative is to use the existing natural gas pipeline network to transport pure or blended

hydrogen-natural gas [3]. However, the big challenge for repurposing the existing gas pipelines is hydrogen embrittlement (HE) that may brittle or degrade the material properties of steel pipelines.

Significant effort has been made to understand the effects of HE on a variety of metals [4, 5]. They have found that HE can result in a substantial loss in ductility and fracture toughness and a decrease of fatigue crack growth resistance or an increase in the fatigue crack growth rate of the metals. This may reduce the overall structural integrity of the metallic material. The loss in structural integrity is in part due to a change in failure mode from a ductile void growth-coalescence mode in air to a more brittle quasi-cleavage mode in hydrogen environments.

In this review, we will focus on the HE effects on the mechanical properties of API pipeline grade steels tested in different hydrogen environments. This includes the yield strength (YS) , ultimate tensile strength (UTS), elongation, reduction of area, fracture toughness, and fatigue crack growth rate (FCGR). There has been an abundance of recent publications in literature investigating HE effects on the mechanical properties of pipeline steels. The literature chosen here was selected to capture the primary contributors to the severity of HE in blended hydrogen-natural gas pipelines. These include the impacts of the pipeline grade, impacts of the microstructure, the amount of hydrogen concentration in the test environment and how the specimen is exposed to it. The common methods to introduce hydrogen into test specimens are discussed first. Followed by a review of how hydrogen affects the tensile properties using different hydrogen charging methods. Then, the HE effects on fracture toughness and fatigue crack growth data are reviewed and analyzed.

2. HYDROGEN CHARGING METHODS

Hydrogen embrittlement in pipeline steel occurs due to exposure to a hydrogen environment. In this environment, the hydrogen enters the steel by first adsorbing onto the surface of the metal and then the atomic hydrogen absorbs into the metal matrix [6]. Researchers have proposed that the presence of hydrogen within the microstructure primarily contributes to HE of pipeline steels through the contributions of two key mechanisms: hydrogen enhanced decohesion (HEDE) and hydrogen enhanced localized plasticity (HELP) [7]. HEDE is a process that weakens the cohesive bonds of the metal in the presence of atomic hydrogen, which increases the likelihood of crack initialization and propagation [8]. Whereas HELP increases localized deformation due to the obstacles that inhibit dislocation motion are reduced in the presence of the atomic hydrogen [9].

To investigate hydrogen effects on mechanical properties, the most often utilized techniques for hydrogen exposure have been either an electrochemical or a gaseous charging process. The electrochemical charging process consists of setting up an electrochemical cell where an electrical charge is passed between the test specimen and a reference electrode that are submerged in an acidic solution [10]. In this setup, the current density, time in the electrochemical cell, the temperature and the electrolyte solution are all important parameters that could impact the amount of hydrogen that is absorbed into the test specimen. For the gaseous charging process, the specimen is placed inside a pressure vessel that is filled and maintained with hydrogen gas. This gas could be pure hydrogen or a blend of hydrogen gas with nitrogen to simulate a blended hydrogen-natural gas mixture. The severity of HE due to the gaseous environment may depend on the amount of hydrogen in the pressure vessel, the purity of the gases, and the temperature. For both cases, the test specimen could be pre-charged and then tested in air or could be charged in situ as the specimen is being tested. However, differences in the severity of HE between pre-charged and in situ charging exist for the electrochemical charging process due to time in the solution and diffusion of the hydrogen back out of the test specimen [11]. Hardie *et al.* [10] has shown that if a pipeline steel specimen is removed from the hydrogen environment and allowed to rest in air, the hydrogen will diffuse back out and the specimen will regain its ductility.

When testing a specimen in a blended hydrogen gas mixture, there are three ways to describe the amount of hydrogen present: the percentage of hydrogen in the blend, the partial pressure of hydrogen, and the hydrogen fugacity (i.e., the “effective pressure” of hydrogen gas, a thermodynamic term). According to Sievert’s law, the steady-state hydrogen concentration in a material is proportional to the square root of the hydrogen fugacity. Since there is a strong correlation between the hydrogen concentration and the severity of HE, then based on Sievert’s law, there is also a direct correlation between the hydrogen fugacity to the severity of HE, as seen in tensile tests that are discussed in section 3.1.1 [12, 13].

Most researchers have chosen electrochemical charging to explore how HE influences the tensile properties of pipeline steels [10, 11, 14-19]. These electrochemical charging methods are less expensive, involve a simpler experimental setup, and are safer since there is no need to use pressurized hydrogen gas. However, a correlation between the HE effects charged with the electrochemical cell and the gaseous hydrogen is needed to enable the use electrochemical charged specimens to provide relevant material mechanical property evaluations. Researchers have proposed to calculate an equivalent fugacity based off the hydrogen concentration found while evaluating the permeation of hydrogen due to electrochemical charging [20, 21]. Their method to determine an equivalent fugacity is as follows. At first, permeation tests are done to calculate the sub-surface hydrogen concentration, for both an electrochemical cell and a specimen undergoing a given pressurized hydrogen gas for several different environmental conditions. Then, using Sieverts’ law the proportional constant (S) between the sub-surface hydrogen concentration and the square root of hydrogen fugacity is determined from a linear regression analysis of the pressurized hydrogen gas permeation tests. This constant is then used to calculate the equivalent fugacity for the electrochemical charging method. An example of the comparison between the sub-surface hydrogen concentration (C_{0R}) as a function of fugacity for gas and electrochemical charging is shown in Fig. 1 for X65 pipeline steel [21]. Following this work, researchers

have started to evaluate mechanical properties of pipeline steel under comparable charging conditions to determine the capability of electrochemical charging for determining the fitness-of-service for pipeline steels in a hydrogen environment [22]. However, there are some limitations with electrochemical charging that need to be addressed. For example, during the electrochemical charging process, the pH value and potential at the crack tip is different than the bulk material [23, 24]. In addition, data suggests a strong time dependence for HE when electrochemically charging specimens [11, 22], while pre-exposure for up to 48 hours in hydrogen gas did not show any additional hydrogen effect [25].

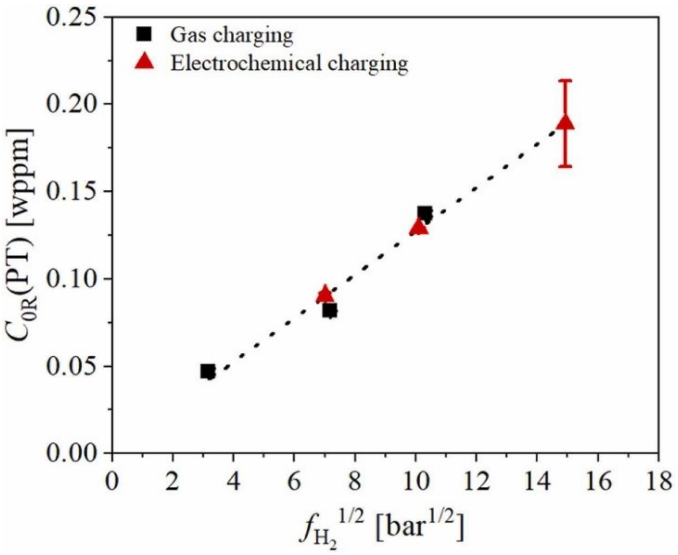

Figure 1. Sub-surface hydrogen concentration C_{0R}(PT) versus the square root of the hydrogen fugacity for both electrochemical and gaseous charging [21].

Recently, researchers have begun to pressurize hollow tubes with hydrogen for a simpler way to test HE effects on the tensile properties of materials [26-31]. While more machining of the specimens would be required, these tests in gaseous hydrogen would be safer than traditional pressure chamber tests due to the lower volume of hydrogen involved during testing. Michler et al. [29] compared the tensile properties in gaseous hydrogen using these tubular and conventional specimens. This review only focuses on the traditional gaseous charging and electrochemical charging tests reported in literature.

3. HYDROGEN EFFECTS ON TENSILE PROPERTIES

When investigating the HE effects on material properties, the mechanical tensile properties, including material tensile strength and ductility, are usually studied first through simple tension tests. ASTM standard E8 [32] provides details on standard specimens and test procedures to measure the material strength in terms of the YS, UTS, and strain hardening exponent (n), and the ductility in terms of the elongation and reduced area at fracture. These tensile properties are the basis for structural limiting design and plastic collapse analysis. For example, the traditional design methods depend on the Barlow model [33] to determine the burst strength based on a single strength measure, namely, the YS or UTS. Recent studies [34] showed that the burst strength of a pipeline depends on the YS and the UTS.

Understanding the HE effects on these tensile properties will enable improved predictions of the burst strength of pipelines carrying pure or blended hydrogen gas. Therefore, this section will review the effects of testing various pipeline steels in a hydrogen environment on their mechanical properties to highlight any trends associated with HE.

3.1 Hydrogen Embrittlement in a gaseous environment

The effects of hydrogen on the mechanical properties of metals have been widely studied over the last century. There are many review papers detailing the effects of hydrogen on a wide variety of metallic materials, most notably being done by Jewett *et al.* [4] and San Marchi and Somerday [5]. Specific research on effects of gaseous hydrogen on the mechanical properties of pipeline steel started in the 1970s with several projects completed by Sandia [25, 35, 36]. In these reports, they tested a variety of pressure vessel and pipeline steels in air and in a hydrogen gas environment at a pressure of 6.9 MPa. Hoover *et al.* [25] reported that gaseous hydrogen had minor effects on YS (8% higher) and UTS (3% higher) of smooth bars for an A106 Gr B pipeline (similar to API 5L Gr B), while an experimental grade X70 showed no effect on YS and UTS. On the other hand, they discovered that the presence of hydrogen significantly affects the ductility, with the ratio between the reduction of area in hydrogen and the reduction of area in air of 86% for the A106 Gr B and 48% for the X70, alongside the elongation to fracture reducing 23% and 15%, respectively, for these two pipeline steels. This showed that the X70 pipeline was more susceptible to HE than the Gr B pipeline.

Holbrook et al. [37] continued the efforts of investigating the effects of hydrogen on the mechanical properties of X42 and X70 in the 1980s at Battelle. They observed a similar effect on the relative reduction of area ratios of 79% for X42 and 82% for X70. However, they reported no reduction in elongation occurring using a 1-inch gauge length, a decrease in the YS between 6% and 10% and a decrease in the UTS of between 2% and 5% in a pure hydrogen environment under a pressure of 6.9 MPa.

These early experiments clearly showed that HE has a minor effect on the YS and UTS, but a significant effect on the ductility of pipeline steels. Other factors that could affect HE on the mechanical properties of pipelines, such as hydrogen pressure, strain rate, purity of the hydrogen, and blended natural gas/hydrogen have been more recently investigated. A review of how these factors influence HE for various grades of pipeline steel is discussed next.

3.1.1 Effects of hydrogen pressure.

Hydrogen pressure's role in HE is crucial to understand when designing pipelines for the transportation of hydrogen gas. One reason is that hydrogen gas has a lower energy density than natural gas, which would require a higher volume of hydrogen

gas to transport the same amount of energy as natural gas, either through larger diameter pipes or higher operating pressures [2]. The impact of hydrogen pressure was investigated by Moro *et al.* [13] and Nanninga *et al*. [12] for pure hydrogen gas at different pressure levels. The stress-strain response for various hydrogen gas pressures is shown in Fig. 2a for a X80 pipeline steel specimen for hydrogen pressures ranging from 0.1 MPa to 30 MPa. Moro *et al.* [13] found that even a small amount of hydrogen gas pressure can result in HE. As the hydrogen pressure increases, a critical limit is reached where a higher hydrogen gas pressure does not result in further ductility reductions. Besides impacts on ductility, small variations in the UTS are observed in these stress-strain curves. Potential causes could be due to experimental variability or the slight effects of varying the total applied hydrogen pressure on the surfaces of the specimen. The most significant effect caused by HE is the reduction in the elongation and reduced area percentages of the smooth tensile specimens. Nanninga *et al.* [12] obtained similar trends on the effects of hydrogen pressure on a X100 pipeline steel for hydrogen gas pressures ranging from 0.2 MPa to 69 MPa. However, as seen in the stress-strain curves in Fig. 2b, there is some scatter in the YS and UTS that is outside the repeatability coefficient of variation reported for a steel material in ASTM E8 [32]. Therefore, it is difficul to conclude on the effect of hydrogen gas pressure on these two strength measures from these experiments. The variations in the ductility measurements are in line with the precision statistics reported in ASTM G142 [38] for Inconel 718 and is dependent on the homogeneity of the material, the surface conditions, and the purity of the hydrogen gas. In addition to the X100 steel, Nanninga *et al*. [12] also tested X52 and X65 and found that the hydrogen effect increased in severity as the strength of the material increased.

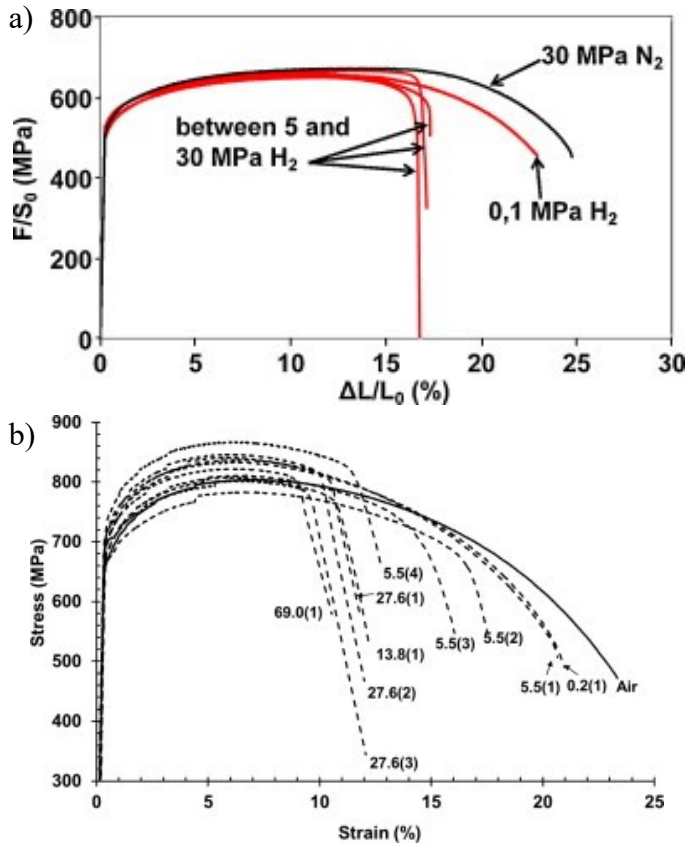

Figure 2. Stress-strain response at various pure hydrogen pressures for (a) X80 [13] and (b) X100 [12]

3.1.2 Effects of hydrogen partial pressure

A key milestone in the transition towards a hydrogen economy is the transportation of blended hydrogen-natural gas through existing natural gas pipelines. Understanding how these blended gases will affect the material properties of the existing pipelines is important. Researchers have recently studied the effects of blended gas pipelines on the strength and ductility of various pipeline grade steels. Nguyen *et al.* [39] tested three different pipeline grades ranging from X42 to X70 in blended hydrogen gas mixtures from 0.1 to 100%.

The resulting stress-strain responses are shown in Fig. 3. For all three materials tested by Nguyen *et al.* [39], the YS and UTS were only slightly affected. For the X42 and X70 pipeline steels, there were insignificant differences in the stress-strain responses for blended gas mixtures of 30% or less hydrogen. While for X65, a significant drop occurred for 30% and then a further drop for the pure 100% hydrogen gas. In a similar study of blended hydrogen gas mixtures, both Meng *et al.* [40] and Wei *et al.* [41] tested X80 pipeline steels for blending ratios between 5 and 50%. They both also reported minimal changes to the YS and UTS as the partial pressure of hydrogen is increased. Wei *et al.* [41] observed the most change in the YS of approximately 3%.

As with the experiments on the effect of hydrogen pressure, these researchers found that as the percentage of hydrogen in blended gas increased, the reduction of the minimal cross-section area and the total elongation decreased. Meng *et al.* [40] and Wei *et al.* [41] both report that all of their tested gas blends starting from 5% hydrogen showed a significant effect on the reduction of the cross-section area and the elongation of API X80 pipeline steel. While Nguyen *et al.* [39] found that the effect of HE on the reduction of the ductility is further dependent on the material [39]. Figure 4 shows how the reduction of cross-section area under various hydrogen blending ratios compares to tests conducted in air [39]. It is seen that for a 0.1% blend of hydrogen, the relative reduction of area (ratio of the reduction of cross-section area in hydrogen to that in air) is approximately 100%, showing that such small blends do not result in a reduction in ductility. Furthermore, the case of X70 steel shows no significant reduction in reduced cross-section area for the three blended gas mixtures of up to 30% hydrogen. Whereas the X42 and X65 steels show a gradual reduction in reduced cross-section area as the precent of hydrogen increases in hydrogen blends above 0.1% hydrogen. Here, X42 performs better than X65 in keeping the amount of reduced cross-section area.

Another contributing factor to the differences in impacts of HE across the three pipeline steel grades is the variation in the

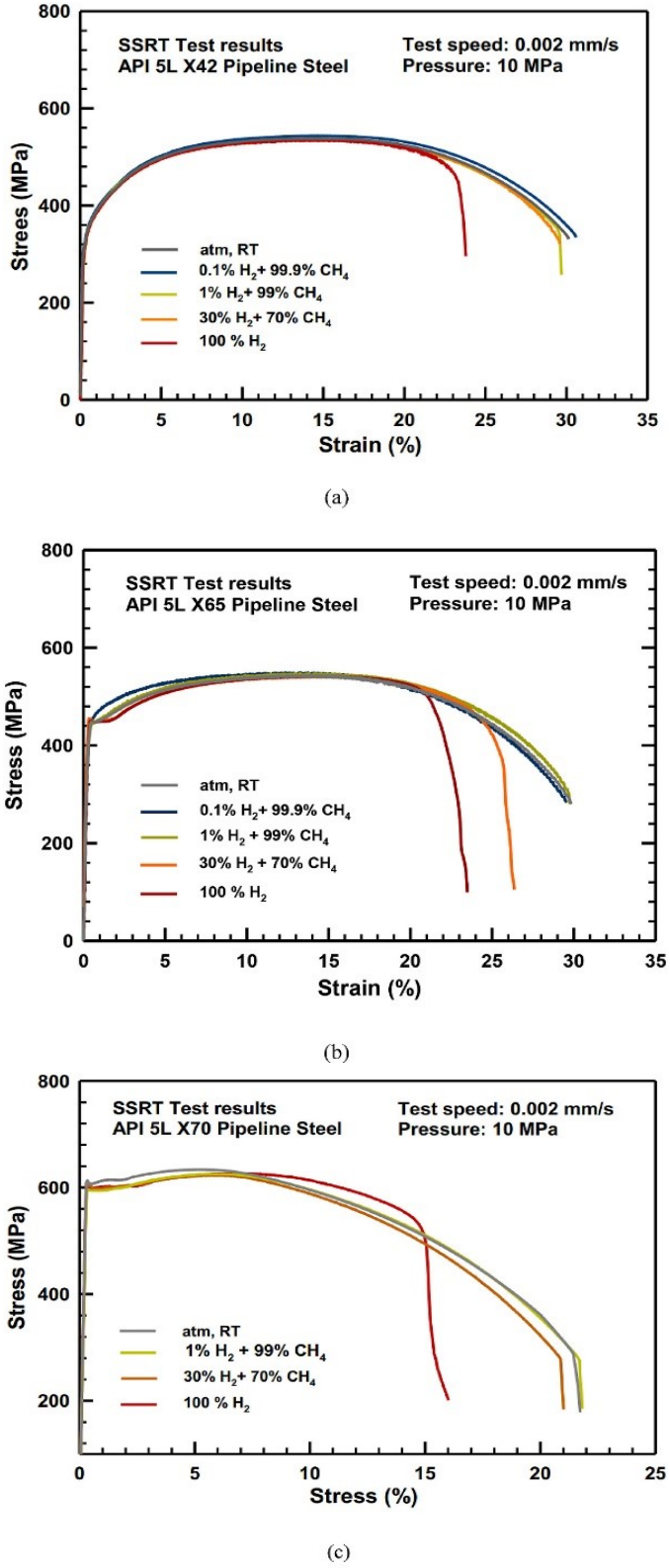

Figure 3. Stress-strain response for three different pipeline steels (a) X42, (b) X65 and (c) X70 in various blended hydrogen-methane environments [39]

microstructure and the amount of observed inclusions. Nguyen *et al.* [39] reports that each of the three steels have varying levels of pearlite, where the X42 steel's microstructure consisted of approximately 23% pearlite and 77% polygonal ferrite, the X65 microstructure consisted of 10% pearlite and 90% polygonal ferite, and the microstructure of the X70 steel consisted of a mix of acicular ferrite, granular ferrite, and bainitic ferrite. Nguyen *et al.* [39] found that the higher susceptibility of X65 steel to HE could be partiailly attributed to the increased number of manganese sulfide inclusisons compared to the other two grades of steel.

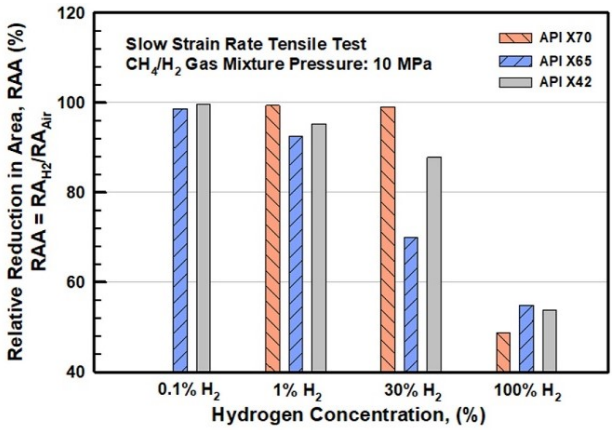

Figure 4. Relative reduction in area of three pipeline steels in various hydrogen gas mixture conditions [39].

3.1.3 Comparing blended and pure hydrogen gas mixtures

The above sections reviewed how both pure hydrogen gas and blended hydrogen-natural gas mixtures significantly impact the ductility of pipeline steels, even at small hydrogen concentrations. There are two related measures of externally applied hydrogen gas to the system: the partial pressure of hydrogen and the hydrogen fugacity. The partial pressure of hydrogen is simply the portion of the total pressure that is due to the amount of hydrogen gas in the mixture. For example, when Nguyen *et al.* [39] used a blended hydrogen-natural gas mixture that consisted of 30% H_2 while applying a total pressure of 10 MPa, the partial pressure of hydrogen applied to the specimen would be 3 MPa. The hydrogen fugacity, f_H, is related to the partial pressure of hydrogen, p_H, and the total pressure, p_T through equation (1),

$$f_H = p_H e^{\frac{b}{RT}p_T} \quad (1)$$

where R is the universal gas constant, T the absolute temperature, and b is a constant representing the finite volume of the gas molecules, which for hydrogen is 15.84 $cm^3\ mol^{-1}$ [42].

To compare the effect of HE across a large body of experiments either of these two measures could determine if there is any significant difference in HE between pure hydrogen and blended hydrogen gas environments. Figure 5 shows the relative reduction of cross-sectional area between that in hydrogen gas and the reference environment (typically air) for

various pipeline grades from Grade B to X100 as a function of hydrogen fugacity. Note that the data in Fig. 5 was collected from literature and includes results of tests in pure hydrogen obtained by Nanninga *et al.* [12] for X100, Moro *et al.* [13] for X80, Hoover *et al.* [25] for A106 Gr B and X70, Holbrook *et al.* [37] for X70 and X80, and Duncan *et al.* [43] for A106 Gr B. In addition, tests in blended hydrogen gas from Nguyen *et al.* [39] for X42, X65 and X70, Meng *et al.* [40] for X80, and Wei *et al.* [41] are also included. The overall trend shows that the effect of HE on the reduced cross-section area is primarily dependent on the hydrogen fugacity and only secondarily on the material grade. There are two phases in this trend with a transition between a hydrogen fugacity between 10 and 20 MPa. Before this transition point there is a sharp reduction in ductility as the hydrogen fugacity increases, while afterwards there is only a small decrease in the relative reduction of cross-sectional area. In addition, there is no discernible difference between a pure hydrogen environment and that of a blended hydrogen gas mixture at the same hydrogen fugacity.

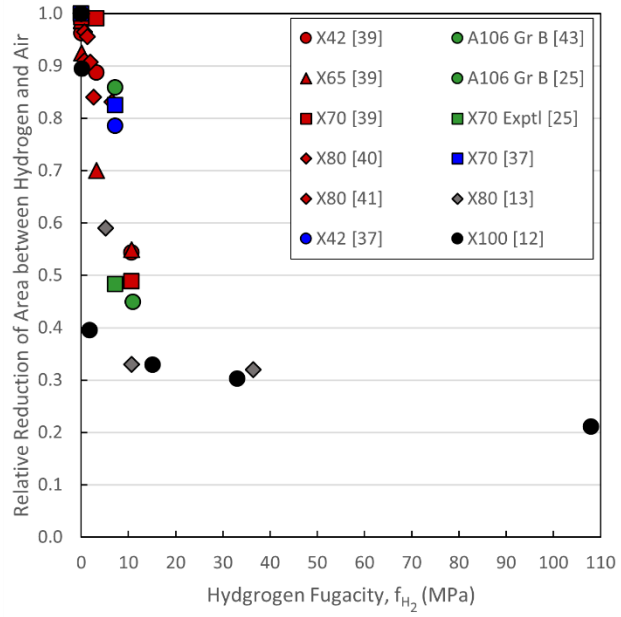

Figure 5. Comparison of the relative reduction of area for various materials as a function of hydrogen partial pressure. The red markers represent the blended hydrogen gas.

3.2 Hydrogen embrittlement in an electrochemical environment

As discussed in Section 2, another way to introduce hydrogen into a material is through immersing the specimen in an electrolyte solution to act as an electrode as current is passed between the specimen and the reference electrode. The main parameters influencing HE of specimens undergoing electrochemical charging include the current density, the pre-charging time, the electrolyte solution and whether the specimens were actively charged throughout the experiment. The influence of these parameters as reported in literature are discussed next.

Some of the earliest electrochemical charging on pipeline steels was reported in Hardie *et al.* [10]. These researchers investigated how the applied charging current density impacted the strength and ductility of three pipeline steels of grades X60 to X100 for a pre-charge time of 15 minutes. Figure 6 shows the variation of the reduction in area with charging current density [10]. These results show a significant loss in ductility for the three steels tested after cathodic charging. The extent of HE is similar across the various pipeline grades tested, except for the highest current density tested where an increase of strength resulted in a higher degree of embrittlement. Hardie *et al.* [10] also reported small decreases (between 2 and 4%) in YS and UTS as the current density increased for the three pipeline steels.

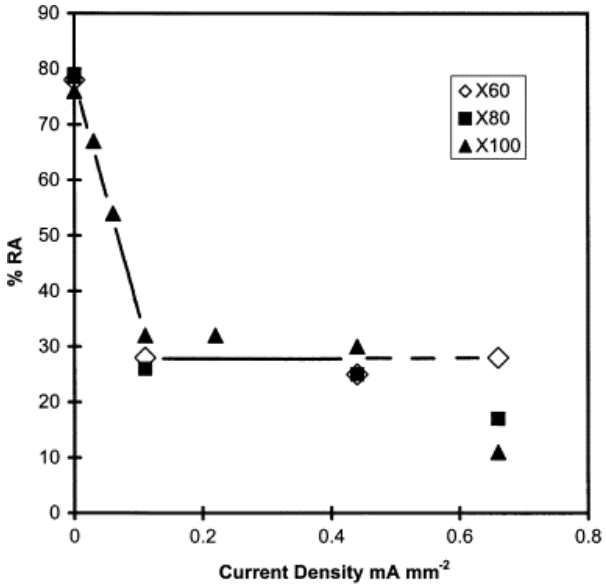

Figure 6. Reduction of cross-sectional area as a function of applied current density for three pipeline grade steels [10].

Han *et al.* [11] explored the effects of charging time and pre-strain levels on HE for X100 steel via electrochemical charging the specimens at a current density of $25\ \mathrm{mA/cm^2}$ in a $0.5\ \mathrm{M}\ H_2SO_4$ solution with $0.5\ \mathrm{g}\ CS(NH_2)_2$ to improve hydrogen atom permeation. They reported that the duration of charging time significantly increased the HE severity, as shown in Fig. 7, by reducing the YS, the UTS and the ductility of the sample. As the hydrogen charging time increased, the efficiency of hydrogen charging resulted in minimal differences in HE for charging times greater than 6 hours. Han *et al.* suggested that the effects of HE were rooted in both the HELP and HEDE mechanisms, with HELP accounting for the decrease of the YS and HEDE promoting more brittle fracture leading to reduced ductility. In addition to the effects of charging time, Han et al. [11] found that the susceptibility to HE increased with pre-straining the specimen prior to charging. They concluded that the dislocations formed due to pre-straining hindered the diffusion of the hydrogen atoms and thus increased the sensitivity of HE.

Cai *et al.* [14] investigated the susceptibility of several different pipeline grade steels to HE using in situ electrochemical

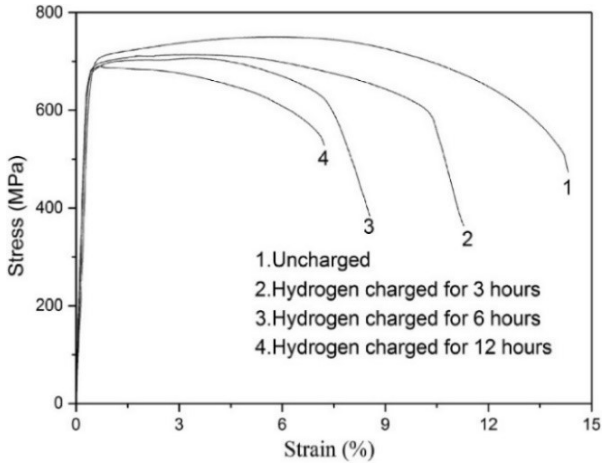

Figure 7. Stress-strain curves of X100 steel under various charging time [11].

hydrogen charging for current densities ranging from 0 to 20 mA cm^{-2}. Figure 8 shows the stress-strain response for the experiments conducted by Cai *et al*. [14]. This figure shows that the severity of HE is dependent on both the material grade and the applied current density. For X42, the stress-strain response shown in Fig. 8a indicates that HE only affected the total elongation, with a higher applied current density leading to a lower strain to failure up to a point where the hydrogen concentration is saturated. On the contrary, for the X70 pipeline steel, the UTS is reduced as the current density increases, with only minimal impacts to the total elongation. The case of X52 has a combination of effects with variations in the YS, the UTS and the strain to failure. In addition to the strain at failure, the researchers measured the reduction of area at failure and found that all three pipeline steels saw a reduction in necking prior to failure for the electrochemical charged specimens. As the hydrogen concentration in the material approaches saturation, the degradation due to hydrogen tends to stabilize resulting in similar levels of reduced cross-sectional areas. These researchers found that for the materials they tested, the HE indexes based on the reduced cross-sectional area of the uncharged and charged specimens are lowest for the X42 grade steel and highest for the X70 [14].

4 HYDROGEN EFFECTS ON FRACTURE TOUGHNESS

Fracture toughness is a measure of a material's resistance to the extension of a crack. Fracture toughness is typically reported in terms of the plane strain fracture toughness (K_{IC}) or the elastic-plastic fracture toughness in terms of the J-integral (J_{IC}). The HE effect on a material's fracture toughness is important to understand so that an adequate fracture toughness due to HE can be measured and an accurate prediction of the critical crack size that would result in failure for a given set of pipeline operating conditions can be determined. The standard ASTM E1820 [44] describes how to determine the fracture toughness of a material using single-edge notched bending (SENB), compact tension (CT), and disk-shaped compact tension (DSCT) specimens.

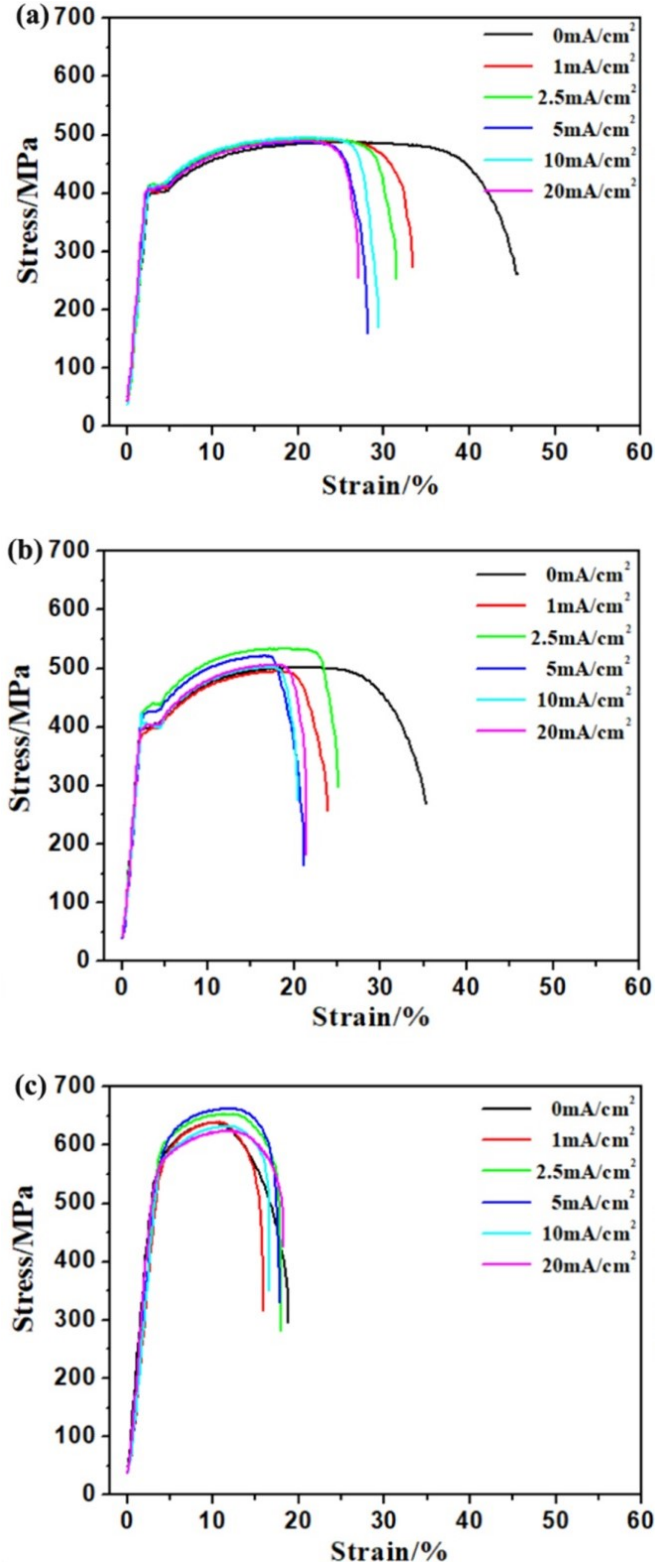

Figure 8. Stress-strain curves for various current density levels for steel pipeline grades (a) X42, (b) X52, and (c) X70 [14].

Representative results from the literature for pipeline steels tested in a hydrogen environment are summarized next.

As previously mentioned, there are two primary ways to force hydrogen uptake into a specimen: electrochemical charging and gaseous pressure chamber. Either of these options can have the hydrogen charged prior to and/or during the experiment. One major downside to electrochemical charging for fracture toughness testing is that since fracture toughness testing takes longer to complete, a portion of the hydrogen could diffuse back out of the metal when tested in air. Such an example is shown in Fig. 9, where the fracture toughness is shown as a function of the current density for pre-charged and in-situ electrochemical charged specimens [45].

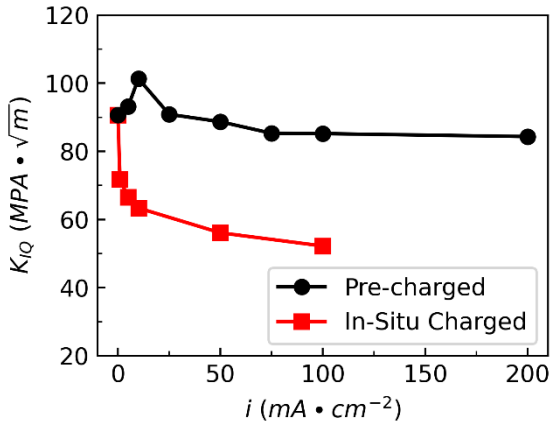

Figure 9. Effect of current density on the fracture toughness under pre-charging (black) for 48 hours and in-situ hydrogen charging (red). Data adapted from Wang [45].

For both cases, the general trend is that as the current density increased (thus a higher amount of hydrogen introduced to the material), the fracture toughness K_{IQ} decreased, where K_{IQ} was converted from J_Q. When comparing the two hydrogen charging methods, the fracture toughness under in situ hydrogen charging is reduced compared to only pre-charging the specimen. This is in part due to the diffusion of hydrogen out of the pre-charged specimens during the experiment, thus lowering the hydrogen concentration. In addition, pH differences inside the crack [23, 24] and an extended charging time can both impact the degree of HE.

Jemblie *et al.* [22] investigated the influence of the hydrogen charging method on the fracture toughness for a modern and a vintage X65 steel. Following the work of Koren *et al.* [21], they determined charging conditions that would result in similar levels of hydrogen fugacity when charging the specimen via an in-situ electrochemical and gaseous charging methods. For the in-situ electrochemical charging, they used a constant potential of -1050mV with Ag/AgCl as the reference electrode in a 3.5 wt.-% NaCl solution and found that the equivalent hydrogen fugacity was dependent on the material with the modern steel having an equivalent hydrogen fugacity of 13.2 bar and 18.2 bar for the vintage. To measure the fracture toughness, they used single edge notch tension (SENT) specimens undergoing a constant increasing displacement rate test to determine the crack tip opening displacement at the maximum load ($CTOD_m$) under similar charging conditions. They found that both charging methods had a lower $CTOD_m$ than in air for both materials, which showed that both materials are susceptible to HE. For a modern X65 material, they found the electrochemical charged specimen had a $CTOD_m$ that was 9.8% lower than the H_2 gas charged sample (Note, there was a 25% difference in fugacity for this condition). While for a vintage X65 material, they found that the electrochemical charged specimen had a $CTOD_m$ that was 6% higher than the H_2 gas charged sample (3% difference in hydrogen fugacity). Some of the difference could have been a result of the methods used to determine $CTOD_m$, since the gas charged sample had no visual access and thus used a single clip gauge to record the crack mouth opening displacement (CMOD).

Jemblie *et al.* [22] also performed a stepwise load increase test and a constant load test under the same in-situ electrochemical charging conditions to find the critical fracture toughness for each method. For the stepwise load increase, the critical fracture toughness was the $CTOD_m$ at failure after increasing the load by 1% and held for 30 minutes until failure. The critical fracture toughness for the constant load test was determined as the highest $CTOD_m$ obtained where fracture does not occur within a holding time of 200 hours. Figure 10 shows the $CTOD_m$ as a function of equivalent hydrogen pressure for all cases, which combines the electrochemical charged results with the hydrogen gas results. They found that the constant load test resulted in a further decrease in the critical $CTOD_m$ by 78% for the modern X65 steel and by 67% for the vintage X65 steel. They suggested that due to the high diffusion rate of pipeline steels, the short diffusion distance, and the constant supply of hydrogen results in a steady state long before the point where failure would occur and therefore mechanisms like creep should be evaluated to see what role they play in impacting the fracture toughness.

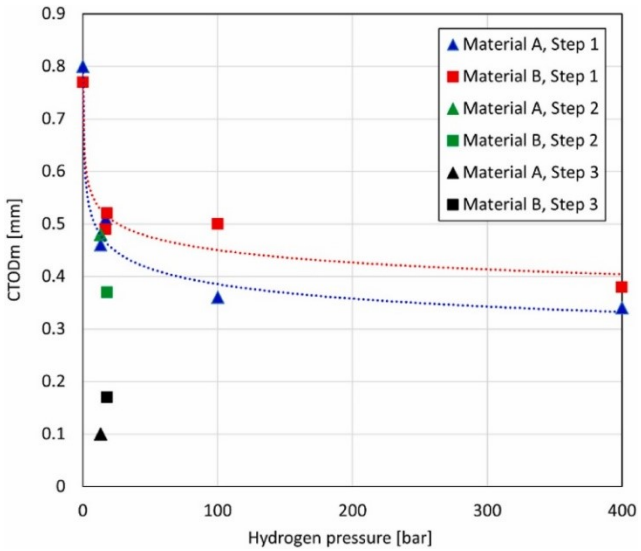

Figure 10. $CTOD_m$ vs hydrogen pressure for Material A (modern X65) and Material B (Vintage X65) [22].

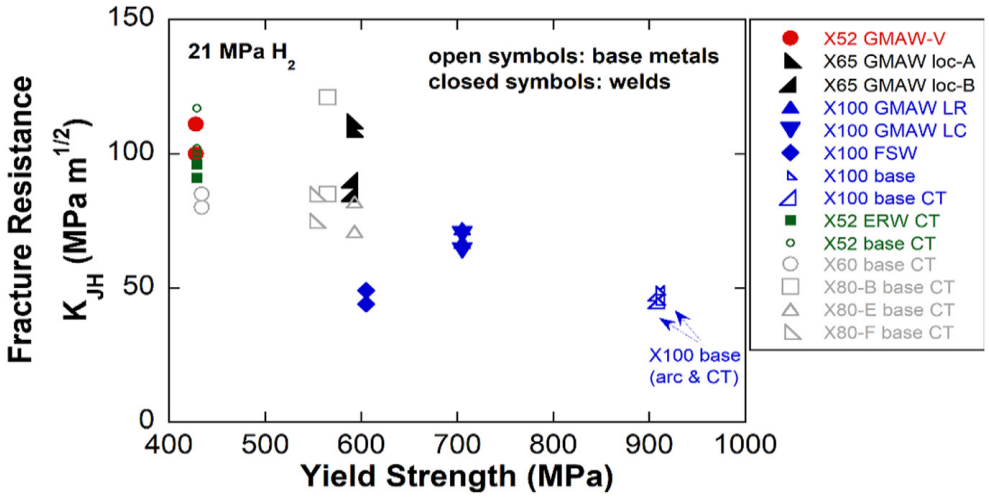

Figure 11. Fracture resistance (K_{JH}) in 21 MPa hydrogen gas as a function of yield strength for pipeline steel welds and base metals [48].

Some of the earliest work investigating the fracture toughness of pipeline steel in hydrogen gas was conducted by Hoover et al. [25, 36] at Sandia in the late 1970's. They tested an X60 steel using a double edge notched tension (DENT) specimen to measure J_{IC}. Performing the tests in 6.9 MPa helium and hydrogen, they found that the hydrogen environment reduced the J_{IC} by approximately 50 and the resistance slope, dJ/da of the J-R curve by a factor of 3.

With the renewed interest in understanding the HE effects on pipeline steels, questions such as how the pipeline grade, microstructure and hydrogen pressure impact the fracture toughness are important to understand for designing new (or repurposing existing) pipelines to transport pure or blended hydrogen gas. This will help accelerate the transition to a hydrogen economy via the safe and economical transport of hydrogen gas.

4.1 Effect of steel grade

The existing natural gas pipeline network consists of different grades of pipeline steels ranging from Gr. B to X80. Understanding how HE effects vary with the material strength or steel grade of the pipeline will provide necessary information on the feasibility of different pipeline grades to transport hydrogen gas. San Marchi *et al.* [46] and Ronevich *et al.* [47] have investigated the fracture resistance of a range of pipeline steels, including X52, X60, X80, and X100. In general, they found that the fracture resistance in high-pressure gaseous hydrogen decreases with the strength of the material, as shown in Fig. 11, where the fracture toughness (K_{JH}) was converted from a size independent, elastic-plastic fracture toughness J-integral (J_H) that was measured in gaseous hydrogen. In addition, Ronevich *et al* [47] found that welds behaved nominally the same as the base metals for the same strength or grade and that K_{JH} is generally greater than 50 MPA$\sqrt{m}$.

Another work done by Agnani *et al.* [48] investigated the HE effects on the fracture toughness of the base material and the weld metal of three different vintage X52 pipeline steels. They also found that in the presence of hydrogen, the fracture toughness decreases for all hydrogen pressure conditions for both the base material and the weld metal, as shown in Fig. 12. As expected, higher hydrogen pressures resulted in lower fracture resistance for all materials and microstructures. In addition, the HE effect was consistent across the various microstructures. The effect of HE occurred in the N62 vintage X52 steel which had the highest amount of carbon and the largest volume fraction of pearlite. Agnani *et al.* [48] conclude that high-local hardness and the inclusion content also contribute to the reduction of fracture resistance.

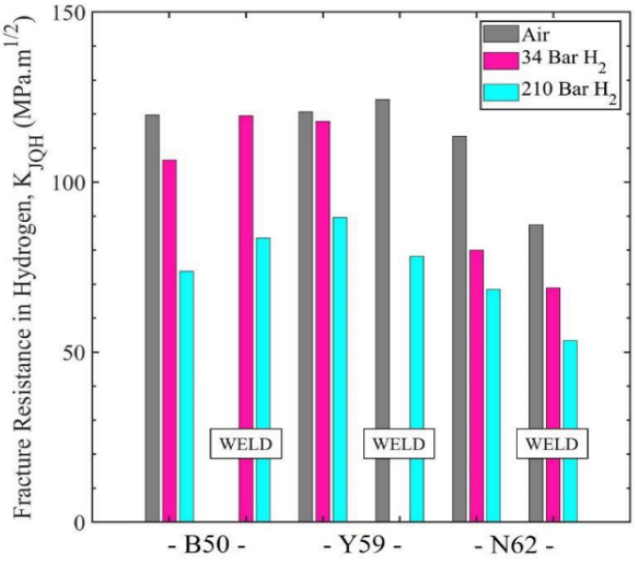

Figure 12. Comparison between fracture resistance of X52 vintage pipeline base metal and weldment in air, 34 bar H_2 and 210 bar H_2 [48].

4.2 Effect of hydrogen pressure

There has been an increasing number of studies investigating the effects of hydrogen pressure or partial hydrogen pressure (when dealing with blended hydrogen-natural gas mixtures) on the fracture toughness of pipeline steels. In one recent study, Nguyen *et al.* [49] investigated the effects of blending 1% hydrogen into natural gas on the fracture toughness of a X70 pipeline steel. They found that even for a minimal amount of hydrogen partial pressure (0.1 MPa), the fracture toughness decreased 25% when compared to air, as shown in Fig. 13, which accounts for approximately half of the reduction in the fracture toughness for the material tested in 100% H_2 at the same total pressure. This follows the overarching trend that as the amount of hydrogen present in the environment increases, the fracture toughness decreases [46, 48, 50, 51].

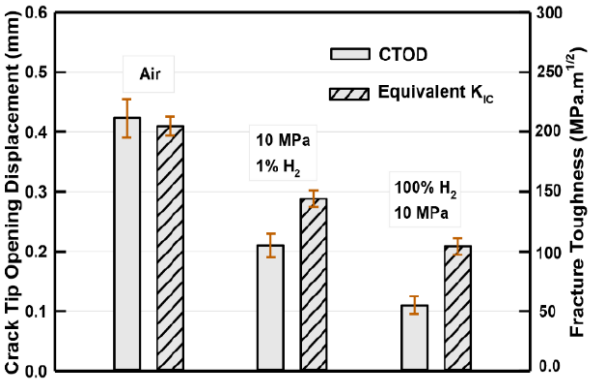

Figure 13. Change in the fracture toughness and fatigue crack growth properties under three hydrogen-containing environments [49].

Agnani *et al.* [51] investigated HE effects on the fracture toughness for different blended hydrogen-natural gas mixtures to identify any trends between hydrogen partial pressure or fugacity and fracture toughness. In addition to the expected non-linear dependance of the fracture toughness on fugacity, the researchers found that even though the fracture toughness of the vintage X52 steel is three times lower than the modern X52 steel, the fracture toughness between them in a hydrogen environment is less than 20% different.

Recently, Ronevich and San Marchi [50] reported the variation of the elastic-plastic fracture resistance K_{JIc} of the X52 pipeline steel with the partial hydrogen pressure, as shown in Fig. 14, where K_{JIc} was converted from the elastic-plastic fracture toughness J_{IC} that was measured in four hydrogen environments of air, N_2-3H_2, and pure hydrogen at a total pressure of 21 and 3.4 MPa. This figure shows that for the X52 pipeline steel, the low partial hydrogen pressure causes a moderate reduction of fracture resistance, and the high hydrogen pressure causes a significant reduction of fracture resistance.

Briottet and Ez-Zaki [52] performed an experimental investigation on the partial hydrogen pressure effect on fracture toughness of an X70 pipeline steel for transporting blended natural gas and hydrogen. The partial hydrogen pressure was

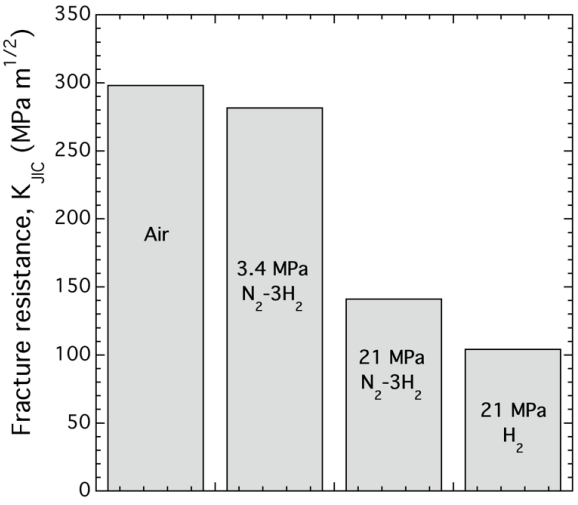

Figure 14. Fracture resistance (KJIC) of X52 pipeline steels in gaseous hydrogen environments [50].

measured as the hydrogen content in a nitrogen (N_2) and hydrogen (H_2) mixture, and the CTOD toughness was measured using standard CT specimens in a high-pressure vessel under a total pressure of 85 bar (8.5 MPa).Four gas mixtures with 0%, 1%, 10%, and 100% H_2 were used, leading to four partial hydrogen pressure of 0, 0.85 bar, 8.5 bar, and 85 bar. Figure 15 shows the relative fracture resistance of the X70 steel in terms of CTOD toughness in the high-pressure vessel under these four cases.

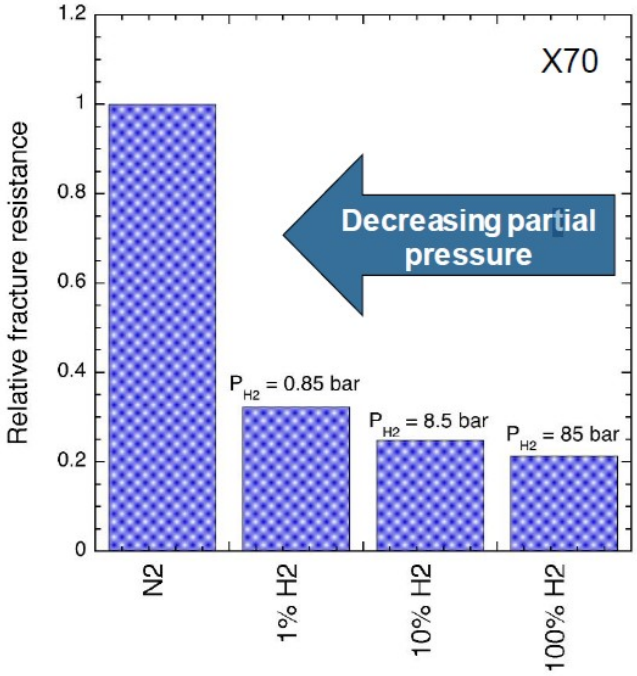

Figure 15. Relative fracture resistance of X70 steel tested in a high-pressure vessel for four hydrogen contents in a total pressure of 85 bar [52].

From this figure, it is observed that 1) the measurements of fracture resistance in gaseous blends of H_2 and N_2 show substantial effects of HE on fracture toughness, 2) a small partial hydrogen pressure (i.e., 1% H_2) is only modestly different than the pure hydrogen (100% H_2), and 3) fracture resistance does not scale linearly with pressure or fugacity.

4.3 Effect of Weld and HAZ Metals

To investigate the impact of HE in weld and heat-affected-zone (HAZ) metals on fracture toughness, Duncan *et al.* [53] performed a series of fracture toughness tests using the C-shaped tensile specimens for A106 Grade B pipeline steel. Crack length was monitored using an alternating DC potential drop system, and J-R curves were constructed from the test data following the ASTM E1820-06 standard. Six C-shaped tensile specimens were machined for the base metal, weld metal, and HAZ material. Half of the specimens from each location were tested in air and the remaining in high-pressure hydrogen gas of 102 atm (i.e., 1500 psig), to measure the J-R curves. The soak time in the hydrogen gas at the pressure was 30 minutes, which was selected based on non-steady state diffusion solution for a plane sheet with a uniform initial distribution and a surface concentration in local equilibrium with the hydrogen at pressure. Figures 16 and 17 show the resulting J-R curves for the base, weld and HAZ material in air and hydrogen. For the base metal, Fig. 16 shows that the J-R curves in hydrogen are significantly lower than those in air. For the weld metal, Fig. 17a shows the J-R curve in hydrogen is significantly lower than in air for one specimen, but comparable J-R curves for the other two specimens. For the HAZ material, Fig. 17b shows that the J-R curves in hydrogen were significantly lower than those in air. As a result, hydrogen may have similar HE effects on the base, weld and HAZ metals.

Recently, Martin et al. [54] analyzed HE effects on the base metal and HAZ metal of X70 pipeline steel in air and in pure hydrogen gas with a pressure 10 MPa. Figure 18 plots the experimental J-R curves measured for the base metal in air, the base metal in 10 MPa hydrogen gas, and the HAZ metal in 10 MPa hydrogen gas. The apparent initial fracture toughness J_Q was determined, as shown in Fig. 19. Figures 18 and 19 show

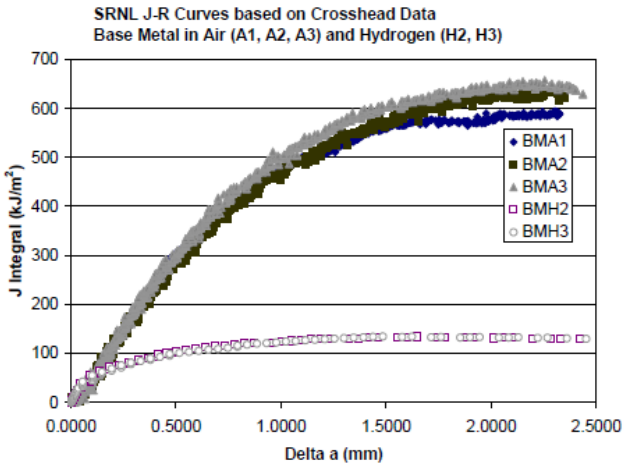

Figure 16. J-R curves measured for the base metal [53].

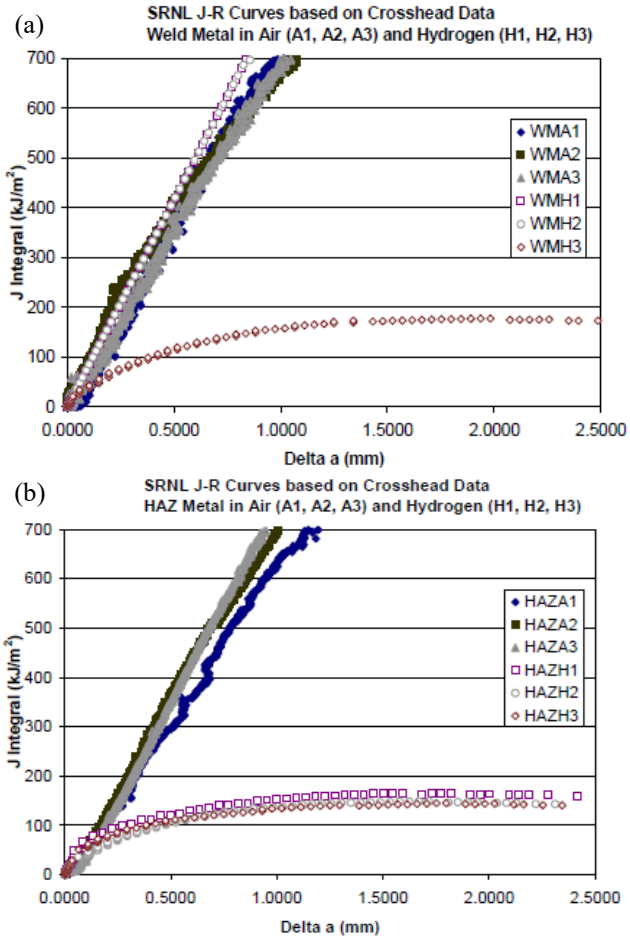

Figure 17. J-R curves measured for the (a) weld metal and (b) HAZ [53].

that the J-R curves and the fracture toughness J_Q are comparable in hydrogen gas for the base and HAZ metal and are significantly lower than when tested in air.

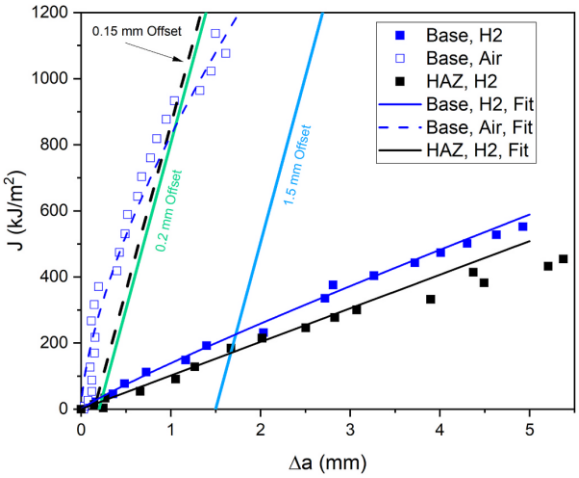

Figure 18. J-R curves measured for base metal and HAZ metal of X70 pipeline steel in air and in 10 MPa hydrogen gas [54].

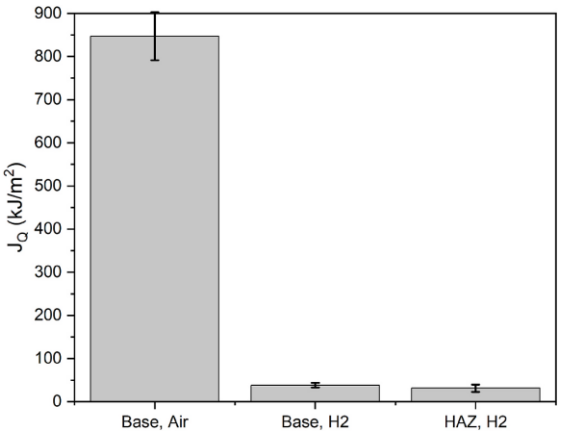

Figure 19. Fracture toughness values of the base in air and in hydrogen and HAZ material in hydrogen gas [54].

5 HYDROGEN EFFECTS ON FATIGUE CRACK GROWTH RATE

The fatigue crack growth rate (FCGR) is a measure of how much a crack will grow under a fatigue loading condition. Alongside the critical crack size that is determined using the fracture toughness, the FCGR is used to evaluate the structural integrity of pipelines by determining the fatigue life. Understanding how HE impacts fatigue crack growth enables the determination of safe design limits for transportation of hydrogen gas thru new and existing pipelines. Cialone and Holbrook [55] investigated HE effects on FCGR of pipeline grade steels. They observed that crack growth rates of a X42 steel in a 6.9 MPa hydrogen gas environment were up to 150 times greater than those with a comparable load in nitrogen. Recent research examining the dependance of the FCGR on hydrogen pressure, stress ratios, material grade and microstructure have led to the development of fatigue design curves for use when evaluating the fitness of service of pipelines transporting hydrogen gas [56-59]. This section will review some of the key results that demonstrate these dependencies.

5.1 Effect of steel grade

San Marchi *et al.* [56] compared FCGR curves for a wide range of pipeline grades, including X42, X60, X70, and X80, as shown in Fig. 20. This figure shows that hydrogen has considerably increased the FCGR for all pipeline grades compared to those in air, and that a wide range of pipeline steels display nominally the same fatigue response in high pressure hydrogen gas except for X42. Recent research has confirmed that material grade only has minimal impactes on hydrogen assisted FCGR for pipeline steels [46, 57-59].

5.2 Effect of hydrogen pressure

Slifka *et al.* [57] investigated the effects of hydrogen pressure on the FCGR for two X52 and two X70 pipeline steels. Figure 21 shows the FCGR under two different hydrogen pressures, as well as in air, for the four pipeline steels. They noted that for all four steels tested, the FCGR was higher as the pressure increased. In addition, they found that when accounting

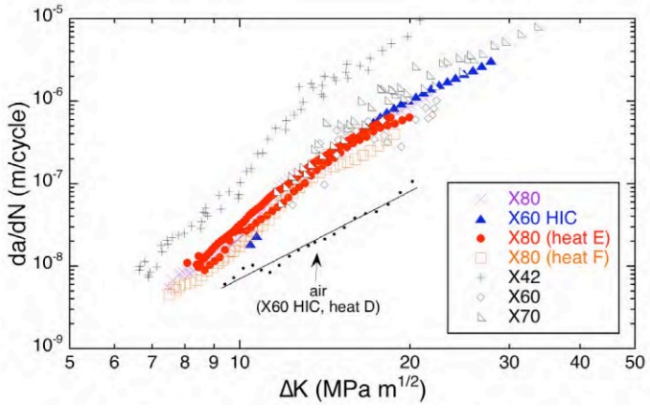

Figure 20. Comparison of fatigue crack growth rate curves for a wide range of pipeline steels from X42 to X80 [56].

for experimental spread, there is minimal differentiation between the FCGRs of the four steels at a constant pressure, which again shows that the FCGR is not dependent on YS. Based on their data, they developed an upper bound phenomenological fatigue crack growth model that encompassed the FCGR data that was implemented in ASME B31.12 [60].

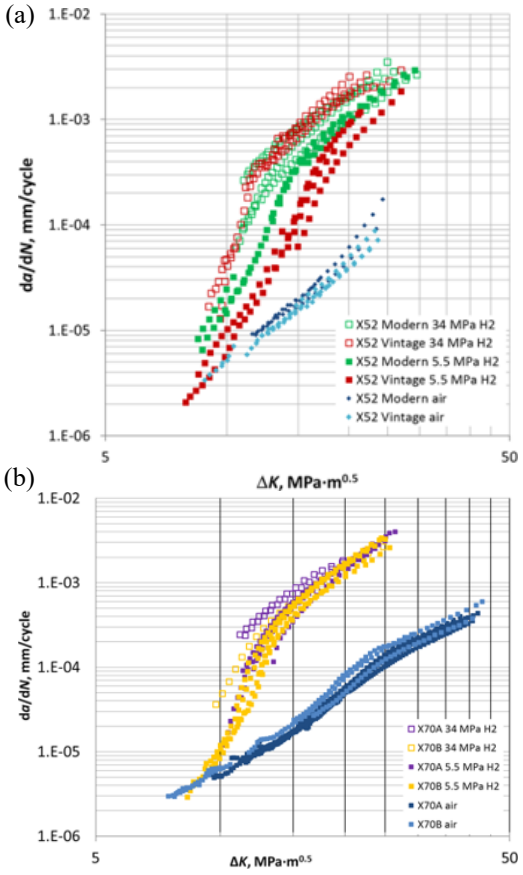

Figure 21. FCGRs on (a) X52 and (b) X70 steels tested at hydrogen gas pressures of 34 MPa (open symbols) and 5.5 MPa (closed symbols), R=0.5, and a cyclic loading rate of 1 Hz. Air data is shown for a baseline FCGR comparison [57].

In addition to the FCGR in pure hydrogen, researchers are also interested in the FCGR for blended hydrogen-natural gas mixtures [40, 49, 50, 51]. Both Nguyen *et al.* [49] and Meng *et al.* [40] found that even for small percentages of hydrogen in the blended gas there was a significant increase in FCGR. However, as seen in Fig. 22, the differences between the four different hydrogen blends were minimal at higher ΔKs. This corresponds with the observations by Slifka *et al.* [57], where the majority of the pressure dependence in the FCGR curves is before the "knee" which typically occurs between values of ΔK of 12 MPa $m^{0.5}$ and 17 MPa $m^{0.5}$, which were not observed in the experiments by Meng *et al*. [40].

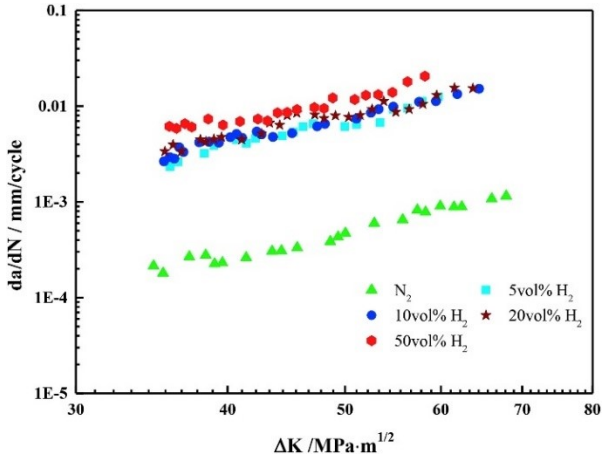

Figure 22. Fatigue crack growth rate curves of an X80 pipeline steel in 5 different environmental conditions [40].

Agnani *et al.* [51] investigated the trends in FCGR for a modern and vintage X52 steel for a wide range of gaseous hydrogen partial pressures. As expected, they observed a substantial dependence on pressure in the fatigue crack growth rate for moderate levels of ΔK (between 10 and 15 MPa $m^{0.5}$). In addition, they compared cases of constant hydrogen partial pressure with cases of constant hydrogen fugacity to determine which variable controlled the HE severity, shown in Fig. 23. For the modern X52 steel (labeled E21), they found minimal difference between the measured rates of fatigue crack growth in pure hydrogen and the two blends. However, for the vintage X52 steel (labeled N62), they found that the higher fugacity condition (3% blend at 1150 bar) displayed higher FCGR than the pure hydrogen, while the partial pressure of hydrogen was the same. These observations showed that hydrogen fugacity correlated well with the trends in FCGR and would be an appropriate environmental parameter to incorporate into fatigue design curves to capture the pressure dependency. Based on this and previous results, San Marchi *et al.* [58] developed an updated two-part fatigue design curve that incorporates the fatigue crack growth rate dependence on pressure and stress ratio.

5.3 Effect of weld and HAZ material

Agnani *et al.* [48] investigated the impact of HE on the FCGR of the weld microstructure of vintage X52 pipeline steels

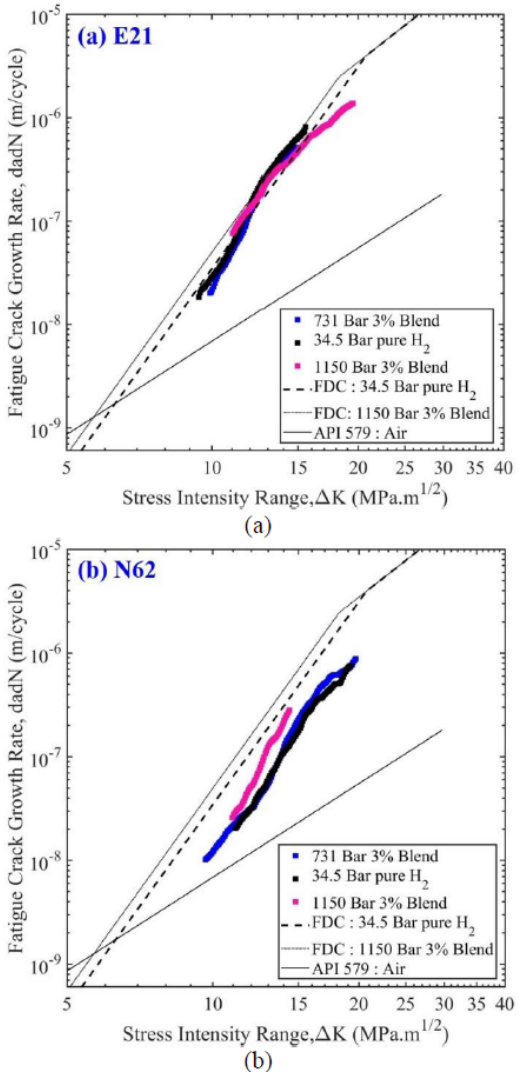

Figure 23. Fatigue crack growth rates of (a) modern E21 steel and (b) vintage N62 steel in pure H_2 and 3% blend with comparable partial pressure and fugacity [51].

and compared the FCGRs to the base metals. Figure 24 shows the comparison of the FCGRs for the base metal and the weld microstructures of the vintage X52 steel (labeled N62) at two different hydrogen pressures. They found that the FCGRs of all the materials and microstructures they tested were bounded by a master design curve. At lower values of ΔK, they found that the base metal and weld microstructures had similar FCGRs and thus similar levels of HE. However, at higher levels of ΔK and before the traditional 'knee', they observed larger scatter in the FCGRs across the vintage base materials and their weld microstructures. This included higher FCGRs for the weld than the base materials, which can be seen in Fig. 24 for ΔK greater than approximately 11 MPa $m^{1/2}$ for a hydrogen pressure of 210 bar, and for a ΔK greater than 12.5 MPa $m^{1/2}$ for a hydrogen pressure of 34 bar. This showed that the weld microstructures are more severely impacted by HE at moderate levels of stress intensity ranges. The stress ratio for all these tests was R=0.5.

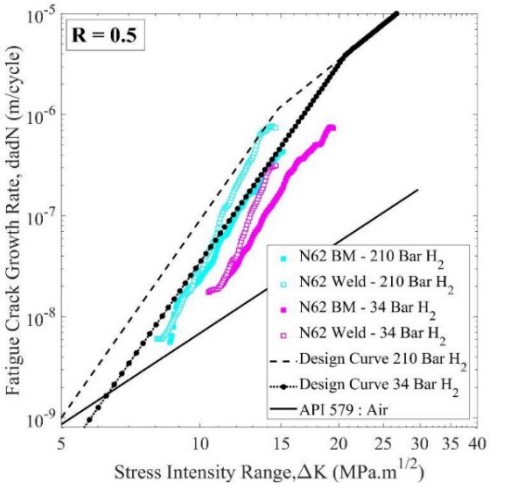

Figure 24. Fatigue crack growth rate versus stress intensity range for vintage X52 pipeline steel base metal and weld microstructures in air and two gaseous hydrogen pressures [48].

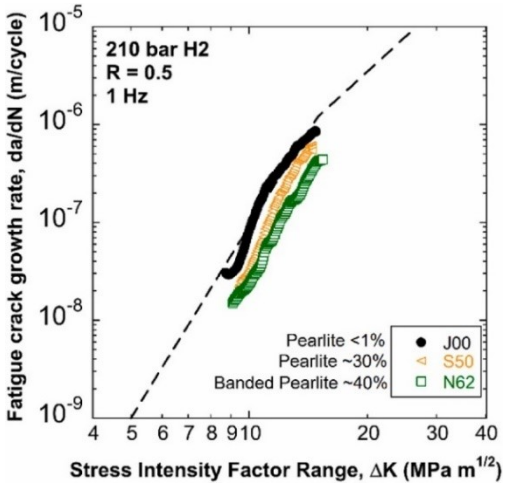

Figure 26. Fatigue crack growth rate for X52 pipeline steels in 210 bar H_2 at R=0.5 with pearlite amounts of <1%, 30%, and 40%. The dashed line represents the FD for this hydrogen partial pressure and stress ratio [59].

5.4 Effect of stress ratio and microstructure

To confirm the fatigue design curves dependance on stress ratios, Ronevich *et al.* [59] compiled fatigue crack growth rates for a modern pipeline steel, a vintage pipeline steel and a pressure vessel at three different stress ratios. Their results, as shown in Fig. 25, indicate that as the stress ratio increases, the FCGR for a given ΔK increased. This trend is captured well by their proposed fatigue design curve shown as the black dashed line in Fig. 25. In addition to the effect of stress ratios, Ronevich *et al.* [59] investigated the effect of microstructure on the FCGR. They used a modern X52 steel with less than 1% pearlite (J00), and two vintage X52 steels with approximately 30% (S50) and 40%(N62) pearlite. Their results, as shown Fig. 26, showed a correlation between the amount of pearlite in the microstructure of the X52 pipeline steels and the FCGRs. They found that lower pearlite percentages resulted in higher FCGRs. They noted that while the vintage steels with higher percentages of pearlite may have had lower FCGRs, the fracture resistance in gaseous hydrogen is inversely proportional to the pearlite fraction.

6 SUMMARY AND OUTLOOK

This paper delivered a technical review of the influences of HE on the tensile, fracture and fatigue properties of pipeline steels. Based on the data collected from the literature, the results showed that gaseous hydrogen charging has a minimal impact on the YS and UTS of the material, while having a significant decrease in the ductility. Initially, the decrease in ductility is rapid as fugacity increases from 0 MPa to approximately 10 MPa. Afterwards, the amount of the reduction in ductility levels out. Similar trends of the decrease in ductility were observed for electrochemical charging when looking at effects of current density. The severity of HE varies with the material grade but has no clear correlation with the material strength. However, the electrochemical pre-charging time usually has a significant effect on the YS, UTS and ductility of pipeline steels.

This review presented the HE effects on fracture toughness for pipeline steels in hydrogen gas environments and discussed the influences of the pipeline steel grade, partial hydrogen pressure, and weld and HAZ metals on the severity of HE. The

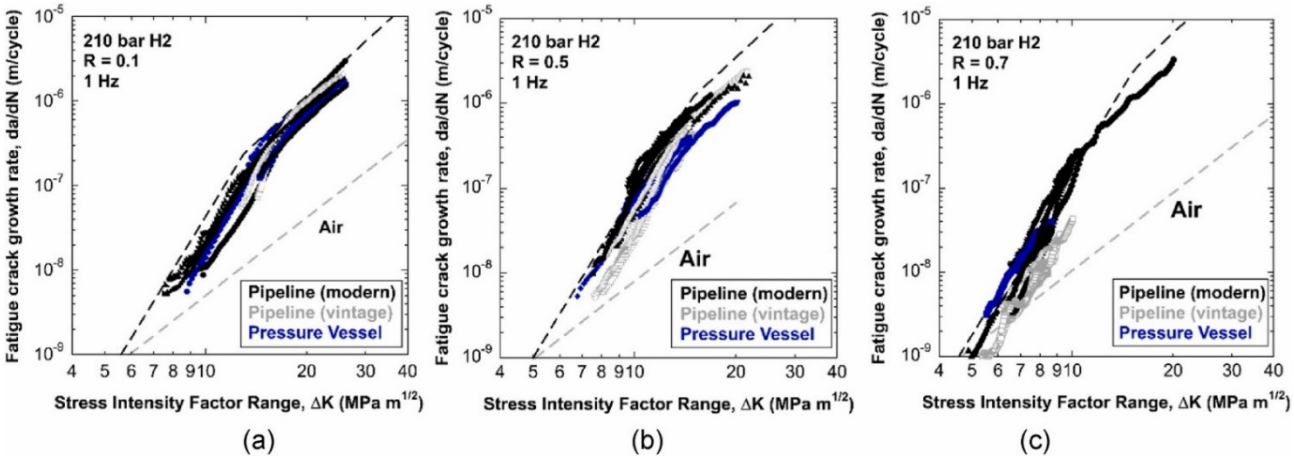

Figure 25. Fatigue crack growth rate curves for pipeline and pressure vessel steels tested in 210 bar hydrogen at stress ratios of: (a) R=0.1, (b) R=0.5, (c) R=0.7 [59].

results showed that the fracture toughness reduces as 1) pipeline steel grade or yield strength increases, and 2) the partial hydrogen pressure increases. Furthermore, the weld and HAZ metals have similar HE effects on fracture toughness as the base metal in hydrogen gas conditions.

This review also presented the HE effects on the FCGR in hydrogen gas environments and discussed the influence of the pipeline steel grade, partial hydrogen pressure, weld and HAZ metals, and microstructure on the severity of HE. It was found that the FCGR significantly increased in hydrogen gas compared to that in air. The results showed that the pipeline grade has a minimal influence on the FCGR in hydrogen gas, and the microstructure has a small effect on the FCGR in hydrogen gas. The impact that HE has on fatigue crack growth curves can be accurately accounted for by using a two-part fatigue design curve that is dependent on the stress ratios, the hydrogen fugacity, and the stress intensity factor range.

Even though extensive investigations on HE have been carried out so far for pipeline steels, further investigations are still needed on this important topic to assess how alternative charging methods compare with traditional gaseous charging methods and to determine more accurate material properties due to hydrogen effects. This includes the YS, UTS, ductility, fracture toughness, and FCGR as a function of the partial hydrogen pressure or the hydrogen fugacity in a hydrogen-natural gas mixture for a wide range of pipeline steel grades from Gr. B to X80. Once these hydrogen-assisted material properties are adequately quantified, accurate assessment models for existing natural gas pipeline steels can be readily improved and remodeled for repurposing these natural gas pipelines to transport blended hydrogen and natural gas.

ACKNOWLEDGEMENTS

This work was produced by Battelle Savannah River Alliance, LLC under Contract No. 89303321CEM000080 with the U.S. Department of Energy. Publisher acknowledges the U.S. Government license to provide public access under the DOE Public Access Plan (http://energy.gov/downloads/doe-public-access-plan). This work was supported by the Laboratory Directed Research and Development (LDRD) program within the Savannah River National Laboratory (SRNL). This document was prepared in conjunction with work accomplished under Contract No. 89303321CEM000080 with the U.S. Department of Energy (DOE) Office of Environmental Management (EM).

REFERENCES

[1] Department of Energy. "U.S. National Clean Hydrogen Strategy and Roadmap." 2023.

[2] Topolski K, et al. "Hydrogen Blending into Natural Gas Pipeline Infrastructure: Review of the State of Technology." Technical Report No. NREL/TP-5400-81704, National Renewable Energy Laboratory, Golden, CO. 2022.

[3] Melaina MW, Antonia O, and Penev M. "Blending Hydrogen into Natural Gas Pipeline Networks: A Review of Key Issues." Technical Report, National Renewable Energy Laboratory, Golden, CO. 2013.

[4] Jewett RP, Walter RJ, Chandler WT, and Frohmberg RP. "Hydrogen Environment Embrittlement of Metals." Contractor Report No. NASA CR-2163, Rocketdyne, Canoga Park, CA. 1973.

[5] San Marchi C, and Somerday BP. "Technical Reference for Hydrogen Compatibility of Materials." Technical Report No. SAND2012-7321, Sandia National Laboratories, Livermore, CA. 2012.

[6] Louthan MR. "Hydrogen Embrittlement of Metals: A Primer for the Failure Analyst." *Journal of Failure Analysis and Prevention,* Vol. 8 No. 3 (2008): 289-307, DOI 10.1007/s11668-008-9133-x.

[7] Ohaeri E, Eduok U, and Szpunar J. "Hydrogen related degradation in pipeline steel: A review." *International Journal of Hydrogen Energy,* Vol. 43 No. 31 (2018): 14584-14617, DOI 10.1016/j.ijhydene.2018.06.064.

[8] Katzarov IH, and Paxton AT. "Hydrogen embrittlement II. Analysis of hydrogen-enhanced decohesion across (111) planes in α-Fe." *Physical Review Materials,* Vol. 1 No. 3 (2017): 1-10, DOI 10.1103/PhysRevMaterials.1.033603.

[9] Birnbaum HK, and Sofronis P. "Hydrogen-enhanced localized plasticity—a mechanism for hydrogen-related fracture." *Materials Science and Engineering: A,* Vol. 176 No. 1 (1994): 191-202, DOI https://doi.org/10.1016/0921-5093(94)90975-X.

[10] Hardie D, Charles EA, and Lopez AH. "Hydrogen embrittlement of high strength pipeline steels." *Corrosion Science,* Vol. 48 No. 12 (2006): 4378-4385, DOI 10.1016/j.corsci.2006.02.011.

[11] Han YD, Wang RZ, Wang H, and Xu LY. "Hydrogen embrittlement sensitivity of X100 pipeline steel under different pre-strain." *International Journal of Hydrogen Energy,* Vol. 44 No. 39 (2019): 22380-22393, DOI 10.1016/j.ijhydene.2019.06.054.

[12] Nanninga NE, et al. "Comparison of hydrogen embrittlement in three pipeline steels in high pressure gaseous hydrogen environments." *Corrosion Science,* Vol. 59 (2012): 1-9, DOI 10.1016/j.corsci.2012.01.028.

[13] Moro I, et al. "Hydrogen embrittlement susceptibility of a high strength steel X80." *Materials Science and Engineering: A,* Vol. 527 No. 27-28 (2010): 7252-7260, DOI 10.1016/j.msea.2010.07.027.

[14] Cai L, et al. "Experimental investigation on the hydrogen embrittlement characteristics and mechanism of natural gas-hydrogen transportation pipeline steels." *Materials Research Express,* Vol. 9 No. 4 (2022): 1-15, DOI 10.1088/2053-1591/ac6654.

[15] Ohaeri E, Eduok U, and Szpunar J. "Relationship between microstructural features in pipeline steel and hydrogen assisted degradation." *Engineering Failure Analysis,* Vol. 96 (2019):496-507, DOI 10.1016/j.engfailanal.2018.11.008.

[16] Ohaeri E, Omale J, Rahman KMM, and Szpunar J. "Effect of post-processing annealing treatments on microstructure development and hydrogen embrittlement in API 5L X70 pipeline steel." *Materials Characterization,* Vol. 161 (2020): 1-18, DOI 10.1016/j.matchar.2020.110124.

[17] Mohtadi-Bonab MA, Masoumi M, and Szpunar JA. "A comparative fracture analysis on as-received and electrochemically hydrogen charged API X60 and API X60SS pipeline steels subjected to tensile testing." *Engineering Failure Analysis,* Vol. 129 (2021): 1-15, DOI 10.1016/j.engfailanal.2021.105721.

[18] Singh V, Singh R, Arora KS, and Mahajan DK. "Hydrogen induced blister cracking and mechanical failure in X65 pipeline steels." *International Journal of Hydrogen Energy,* Vol. 44 No. 39 (2019): 22039-22049, DOI 10.1016/j.ijhydene.2019.06.098.

[19] Rahman M, et al. "Effect of electrochemical hydrogen charging on an API X70 pipeline steel with focus on characterization of inclusions." *International Journal of Pressure Vessels and Piping,* Vol. 173 (2019): 147-155, DOI 10.1016/j.ijpvp.2019.05.006.

[20] Venezuela J, et al. "Equivalent hydrogen fugacity during electrochemical charging of some martensitic advanced high-strength steels." *Corrosion Science,* Vol. 127 (2017): 45-58, DOI 10.1016/j.corsci.2017.08.011.

[21] Koren E, et al. "Experimental comparison of gaseous and electrochemical hydrogen charging in X65 pipeline steel using the permeation technique." *Corrosion Science,* Vol. 215 (2023): 1-10, DOI 10.1016/j.corsci.2023.111025.

[22] Jemblie L, et al. "Safe pipelines for hydrogen transport." *International Journal of Hydrogen Energy,* In Press (2024): 1-14, DOI 10.1016/j.ijhydene.2024.06.309.

[23] Chandra A, Thodla R, Tylczak J, and Ziomek-Moroz M. "Fatigue and Static Crack Growth Rate Study of X-65 Line Pipe Steel in Gas Transmission Pipeline Applications." *Proceedings of the CORROSION 2021,* NACE-2021-16721. Virtual, April 19, 2021.

[24] Li Y, Liu Z, Fan E, Cui Z, and Zhao J. "The effect of crack tip environment on crack growth behaviour of a low alloy steel at cathodic potentials in artificial seawater." *Journal of Materials Science & Technology,* Vol. 54 (2020): 119-131, DOI https://doi.org/10.1016/j.jmst.2020.04.034.

[25] Hoover WR, Robinson SL, Stoltz RE, and Spingam JR. "Hydrogen Compatibility of Structural Materials for Energy Storage and Transmission Final Report." Technical Report No. SAND81-8006, Sandia National Laboratories, Livermore, CA. 1981.

[26] Hejazi D, Calk, A, Dunne D, and Pereloma E. "Effect of gaseous hydrogen charging on the tensile properties of standard and medium Mn X70 pipeline steels." *Materials Science and Technology,* Vol. 32 No. 7 (2016): 675-683, DOI 10.1080/02670836.2015.1130331.

[27] Freitas T, et al. "Tensile testing in high-pressure gaseous hydrogen using the hollow specimen method." *MRS Bulletin,* Vol. 49 (2024): 1-9, DOI 10.1557/s43577-024-00776-9.

[28] Campari A, Konert F, Sobol O, and Alvaro A. "A comparison of vintage and modern X65 pipeline steel using hollow specimen technique for in-situ hydrogen testing." *Engineering Failure Analysis,* Vol. 163 (2024): 1-15, DOI 10.1016/j.engfailanal.2024.108530.

[29] Michler T, Ebling F, Oesterlin H, Fischer C, and Wackermann K. "Comparison of tensile properties of X60 pipeline steel tested in high pressure gaseous hydrogen using tubular and conventional specimen." *International Journal of Hydrogen Energy,* Vol. 47 No. 81 (2022): 34676-34688, DOI 10.1016/j.ijhydene.2022.07.211.

[30] Boot T, et al. "In-Situ Hollow Sample Setup Design for Mechanical Characterisation of Gaseous Hydrogen Embrittlement of Pipeline Steels and Welds." *Metals,* Vol. 11 No. 8 (2021): 1-16, DOI 10.3390/met11081242.-

[31] Walallawita, R, et al. "Evaluating the Effect of Blended and Pure Hydrogen in X60 Pipeline Steel for Low-Pressure Transmission Using Hollow-Specimen Slow-Strain-Rate Tensile Testing." *Metals,* Vol. 14 No. 10 (2024): 1-13, DOI 10.3390/met14101132.

[32] ASTM E8/E8M-24. *Standard Test Methods for Tension Testing of Metallic Materials.* ASTM International, West Conshohocken, PA, 2024.

[33] Zhu X-K. "A comparative study of burst failure models for assessing remaining strength of corroded pipelines." *Journal of Pipeline Science and Engineering,* Vol. 1 No. 1 (2021): 36-50, DOI 10.1016/j.jpse.2021.01.008.

[34] Zhu X-K, and Leis BN. "Average shear stress yield criterion and its application to plastic collapse analysis of pipelines." *International Journal of Pressure Vessels and Piping,* Vol. 83 No. 9 (2006): 663-671, DOI 10.1016/j.ijpvp.2006.06.001.

[35] Robinson SL. "Hydrogen Compatibility of Structural Materials for Energy Storage and Transmission Applications (Semiannual Reprot for Period Through October 1, 1976)." Technical Report No. SAND76-8255, Sandia National Laboratories, Livermore, CA. 1976.

[36] Hoover WR. "Hydrogen Compatibility of Structural Materiasl for Energy Storage and Transmission." Technical Report No. SAND79-8200, Sandia National Laboratories, Livermore, CA. 1979.

[37] Holbrook JH, Cialone HJ, and Scott PM. "Hydrogen Degradation of Pipeline Steels Summary Report." Technical Report No. BNL-51855, Battelle Memorial Institute, Columbus, OH. 1984.

[38] ASTM G142-98. *Standard Test Methods for Determination of Susceptibility of Metals to Embrittlement in Hydrogen Containing Environments at High Pressure, High Temperature, or Both.* ASTM International, West Conshohocken, PA, 2022.

[39] Nguyen TT, Bae K-O, Jaeyeong P, Nahm SH, and Baek UB. "Damage associated with interactions between microstructural characteristics and hydrogen/methane gas mixtures of pipeline steels." *International Journal of Hydrogen Energy,* Vol. 47 No. 73 (2022): 31499-31520, DOI 10.1016/j.ijhydene.2022.07.060.

[40] Meng B, et al. "Hydrogen effects on X80 pipeline steel in high-pressure natural gas/hydrogen mixtures." *International Journal of Hydrogen Energy,* Vol. 42 No. 11 (2017): 7404-7412, DOI 10.1016/j.ijhydene.2016.05.145.

[41] Wei H, et al. "Influence of hydrogen in natural gas mixed hydrogen environment on mechanical properties of X80 pipeline steel." *International Journal of Hydrogen Energy,* Vol. 54 (2024): 908-921, DOI 10.1016/j.ijhydene.2023.09.138.

[42] San Marchi C, Somerday B, and Robinson S. "Permeability, solubility and diffusivity of hydrogen isotopes in stainless steels at high gas pressures." *International Journal of Hydrogen Energy,* Vol. 32 No. 1 (2007): 100-116, DOI 10.1016/j.ijhydene.2006.05.008.

[43] Duncan A, Lam P, and Adams T. "Tensile Testing of Carbon Steel in High Pressure Hydrogen." *Proceedings of the ASME 2007 Pressure Vessels and Piping Conference* PVP2007-26736. San Antonio, Texas, USA, July 22–26, 2007.

[44] ASTM E1820-24. *Standard Test Method for Measurement of Fracture Toughness.* ASTM International, West Conshohocken, PA, May, 2024.

[45] Wang D, et al. "Investigation of hydrogen embrittlement behavior in X65 pipeline steel under different hydrogen charging conditions." *Materials Science and Engineering: A,* Vol.860 (2022): 1-10, DOI 10.1016/j.msea.2022.144262.

[46] San Marchi C, Shrestha R, and Ronevich J. "Hydrogen Compatibility of Structrual Materials in Natural Gas Networks." *Proceedings of the International Conference on Hydrogen Safety*. Edinburgh, Scotland, September 24th, 2021.

[47] Ronevich JA, Song EJ, Somerday BP, and San Marchi CW. "Hydrogen-assisted fracture resistance of pipeline welds in gaseous hydrogen." *International Journal of Hydrogen Energy,* Vol. 46 No. 10 (2021): 7601-7614, DOI 10.1016/j.ijhydene.2020.11.239.

[48] Agnani M, et al. "Fatigue and Fracture Behavior of Vintage Pipelines in Gaseous Hydrogen Environment." *Proceedings of the ASME 2023 Pressure Vessels & Piping Conference,* PVP2023-105622. Atlanta, Georgia, July 16-21, 2023.

[49] Nguyen TT, Heo HM, Park J, Nahm SH, and Beak UB. "Fracture properties and fatigue life assessment of API X70 pipeline steel under the effect of an environment containing hydrogen." *Journal of Mechanical Science and Technology,* Vol. 35 No. 4 (2021): 1445-1455, DOI 10.1007/s12206-021-0310-0.

[50] Ronevich JA, and San Marchi C. "Materials Compatibility Concerns for Hydrogen Blended Into Natural Gas." *Proceedings of the ASME 2021 Pressure Vessels & Piping Conference,* PVP2021-62045. Virtual, Online, July 13-15, 2021.

[51] Agnani M, Ronevich JA, and San Marchi C. "Comparison Between Fatigue and Fracture Behavior of Pipeline Steels in Pure and Blended Hydrogen at Different Pressures." *Proceedings of the ASME 2024 Pressure Vessels & Piping Conference,* PVP2024-123477. Bellevue, Washington, July 28 - August 2, 2024.

[52] Briottet L, and Ez-Zaki H. "Influence of Hydrogen and Oxygen Impurity Content in a Natural Gas / Hydrogen Blend on the Toughness of an API X70 Steel." *Proceedings of the ASME 2018 Pressure Vessels and Piping Conference,* PVP2018-84658. Prague, Czech Republic, July 15-20, 2018.

[53] Duncan AJ, Adams TM, and Lam P-S. "Fracture Property Testing of Carbon Steel in High Pressure Hydrogen." *Proceedings of the ASME 2009 Pressure Vessels and Piping Conference,* PVP2009-78069: 225-231. Prague, Czech Republic, July 26-30, 2009.

[54] Martin ML, Connolly M, Buck ZN, Bradley PE, Lauria D, and Slifka AJ. "Evaluating a natural gas pipeline steel for blended hydrogen service." *Journal of Natural Gas Science and Engineering,* Vol. 101 (2022): 1-6, DOI 10.1016/j.jngse.2022.104529.

[55] Cialone HJ, and Holbrook JH. "Sensitivity of Steels to Degradation in Gaseous Hydrogen." *Hydrogen Embrittlement: Prevention and Control.* American Society for Testing and Materials, West Conshohocken, PA, 1988: pp. 134-152.

[56] San Marchi C, et al. "Fracture Resistance and Fatigue Crack Growth of X80 Pipeline Steel in Gaseous Hydrogen." *Proceedings of the ASME 2011 Pressure Vessels and Piping Conference,* PVP2011-57684. Baltimore, Maryland, July 17-21, 2011.

[57] Slifka AJ, Drexler ES, Amaro RL, Hayden LE, Stalheim DG, Lauria DS, and Hrabe NW. "Fatigue Measurement of Pipeline Steels for the Application of Transporting Gaseous Hydrogen." *Journal of Pressure Vessel Technology,* Vol. 140 No. 1 (2018): 1-12, DOI 10.1115/1.4038594.

[58] San Marchi C, Ronevich JA, Bortot P, Ortolan, M, Xu K, and Rana M. "Technical Basis for Fatigue Crack Growth Rules in Gaseous Hydrogen for ASME B31.12 Code Case 220 and for Revision of ASME VIII-3 Code Case 2938-1." *Proceedings of the ASME 2024 Pressure Vessels & Piping Conference,* PVP2024-122529. Bellevue, Washington, July 28-August 2, 2024.

[59] Ronevich, J, Agnani, M, and San Marchi, C. "Consistency of fatigue crack growth behavior of pipeline and low-alloy pressure vessel steels in gaseous hydrogen." *International Journal of Hydrogen Energy,* In Press (2024): 1-9, DOI 10.1016/j.ijhydene.2024.06.287.

[60] ASME B31.12-2023. *Hydrogen Piping and Pipelines.* The American Society of Mechanical Engineers, New York, NY, December 29, 2023